

# A Low Noise Thermoelectric Infrared Detector Microsystem in a Digital CMOS Technology

Christian Menolfi, Qiuting Huang and Niklaus Schneeberger\*

Integrated Systems Laboratory, \* Physical Electronics Laboratory, ETH Zürich  
Gloriastr. 35, CH-8092 Zürich, Switzerland

## Abstract

A low noise sensor interface for low-frequency thermoelectric infrared sensor applications is described which uses chopper technique to reduce low-frequency noise and offset. The circuit has been integrated in a transistor-only 1  $\mu\text{m}$  single-poly, n-well CMOS process. It features a gain of 52 dB with a 500 Hz bandwidth and a CMRR of more than 70 dB. The equivalent input noise is 15  $\text{nV}/\sqrt{\text{Hz}}$  and free from  $\frac{1}{f}$ -noise. The input offset is 1.5  $\mu\text{V}$  for a tuning error of less than 4%. The resulting sensor system allows the detection of a minimum required radiation signal of below 120  $\text{nW}/\text{mm}^2$ . The amplifier consumes 1.3  $\text{mW}$ .

## Introduction

Continuing progress in processing technologies in recent years have stimulated rapid development of integrated micro-sensors, in which a notable trend is to realize intelligent sensors with the same technologies as the integrated circuits. Combining sensors and circuits in a circuit technology such as CMOS makes the resulting micro-system competitive in price by tapping the strong manufacturing base of the IC technologies, which have perfected themselves in low cost mass production, and by reducing the complexity and cost for packaging. Sensors implemented in a standard (CMOS) circuit technology, however, tend to have lower sensitivity than those implemented in specialized sensor technologies. This loss in performance must be made up by the “co-integrated” interface electronics, which often makes the design of the latter a challenging task. In this contribution we present a highly sensitive sensor interface for CMOS compatible thermoelectric infrared (IR) radiation sensors for intrusion detection applications.

## Thermoelectric IR Sensors

Thermoelectric IR sensors can be built as shown in the schematic of fig. 1. The device consists of a thermally insulated absorbing area which will convert the incident radiation into heat. This temperature increase can be detected using a thermopile consisting of polysilicon/aluminum thermocouples which sense the temperature difference between its “hot” junctions on the absorbing area and the “cold” junctions lying on the silicon bulk. The absorbing area is an oxide/nitride membrane which is obtained by anisotropic etching of the silicon bulk from the backside of the wafer. The output voltage  $V_T$  of the thermopile is given by  $V_T = N \times \alpha \times \Delta T$ , where  $N$ ,  $\alpha$  and  $\Delta T$  denote the number of thermocouples, the Seebeck coefficient and the temperature difference between the hot and cold junction, respectively. Two figures of merit for thermoelectric IR sensors are the responsivity  $S$  and the noise equivalent power  $NEP$ . The responsivity  $S$  in  $[\text{V}/\text{W}]$  is defined as the sensor output voltage  $V_T$  divided by the total integrated incident radiation power on the membrane. The  $NEP$  in  $[\text{W}/\sqrt{\text{Hz}}]$  is the radiation power required for a S/N ratio of 1 over a 1 Hz bandwidth at the sensor output:  $NEP = \sqrt{4kTR_T}/S$ , where  $R_T$  denotes the thermopile resistance. Optimization of the  $NEP$  for a given membrane size can be carried out using finite element simulation [1]. At first sight increasing the number of thermocouples for a given membrane area would also increase the sensor readout signal  $V_T$  and the responsivity  $S$ . However, the thermal conductivity of the thermopile (which is dominated by the conductivity of the metal) will be increased by the same amount. The temperature difference  $\Delta T$  therefore decreases leaving the responsivity  $S$  of the sensor to a first order constant. This implies that low impedance thermopiles will have better  $NEP$  than high impedance thermopiles, but also, that a low noise amplifier is required which does not affect

the sensor's resolution. In our case the amplifier should cope with thermopile resistors ranging from  $20\text{ k}\Omega$  . . .  $200\text{ k}\Omega$ , which sets its equivalent low frequency input noise to about  $15\text{ nV}/\sqrt{\text{Hz}}$ .

Possible applications of thermoelectric IR sensors include remote temperature sensors, building control and intrusion detection. In the latter case minimum radiation power of typically  $120\text{ nW}/\text{mm}^2$  has to be detected which results in barely 1 microvolt sensor readout in an application specific 10 Hz bandwidth. To avoid saturation of the amplifier stage its offset should be in the same range. In detector applications an optical mirror system usually focuses the incoming radiation on two differentially connected IR sensors such that common mode background radiation will be cancelled out. The data of the sensor optimized for this application is summarized in fig. 3. Fig. 2 shows a photograph of the sensor membrane.

### Low Noise Circuit Techniques

Typical conventional CMOS amplifiers are known for their high  $\frac{1}{f}$ -noise and offset. To reach the desired low-frequency noise level of  $15\text{ nV}/\sqrt{\text{Hz}}$  and offset in the microvolt range special circuit techniques must be employed. One way to reduce low-frequency noise is the auto-zero technique [2, 3]. Although  $\frac{1}{f}$ -noise can be substantially reduced, residual offset due to charge injection of the switches will still remain. Furthermore the thermal noise of the amplifier will be increased due to under-sampling of broad-band noise. In contrast to the auto-zero technique, no noise undersampling occurs in the chopper amplifier principle [4, 5]. The input signal is modulated by a square-wave signal with frequency  $f_{chop}$ , mixing it to the odd harmonics of  $f_{chop}$ . It is then amplified and modulated back to the baseband. The noise and offset are only modulated once by the output multiplier and translated to the odd harmonics of  $f_{chop}$ . By using a selective filter/amplifier most of the input modulator's charge injection signal can be filtered which results in a very low residual offset in the microvolt range [5].

### Circuit Implementation

The block diagram of the implemented interface system is shown in fig. 4. The system consists of an input modulator, a low noise preamplifier, a second order bandpass filter and an output modulator. To allow operation in a mixed-signal environment the signal path throughout the whole amplifier has been kept fully differential to reject power supply related signals on the one hand and to suppress charge injection of the input switches on the other [2]. Furthermore, even order distortion terms will be reduced. Both modulators are driven with the same clock.

The preamplifier depicted in fig. 5 is the very low noise front end. To optimize the input stage a trade-off between  $\frac{1}{f}$ -noise performance on the one hand and residual offset on the other had to be found. The chopper frequency has been chosen to be at the  $\frac{1}{f}$ -noise corner frequency which is around  $5\text{ kHz}$ . The equivalent input impedance will become more than  $100\text{ M}\Omega$ . The gain of the amplifier is determined by the ratio of two PMOS transconductors which provides sufficient gain accuracy for most microsensor applications. To increase the maximal output signal, the output transconductor has been linearized [6]. The second order bandpass filter with center frequency locked to  $f_{chop}$  represents the second gain stage of the chopper system and is the key element for low residual offset. Due to its selective behavior most of the unwanted clock feed-through signal components, which are located at multiples of  $f_{chop}$  and are responsible for a residual offset, will be attenuated to a large extent. However, larger residual offset is expected for larger thermopile resistors  $R_T$  [5]. The filter is centered at  $5\text{ kHz}$  with a gain of 25 at resonance and a Q of 5. This results in a  $500\text{ Hz}$  equivalent signal bandwidth for the chopper amplifier. Although a higher Q would be desirable to maximize the gain, the higher Q will also demand a very accurate tuning of the chopping frequency  $f_{chop}$  to the center frequency of the filter in order to avoid gain error. A Q of 5 is a good trade-off between amplifier gain accuracy and clock feedthrough signal attenuation. The filter has been realized using the Gm-C technique (fig. 7). The schematic of the integrator is shown in fig. 6. It uses linearized transconductors and grounded NMOS as capacitors. Due to the use of grounded MOS a degradation of the negative PSRR at higher frequency must be taken into account, however, they are an area efficient solution in a transistor-only standard CMOS process.

### Experimental results

A test chip with the circuit has been fabricated in a standard digital  $1\text{ }\mu\text{m}$  CMOS process. The chip photograph is shown in fig. 8. The core area is  $1260\text{ }\mu\text{m} \times 1110\text{ }\mu\text{m}$ . Fig. 9 summarizes the performance

of the interface system. Fig. 10 shows the frequency response of the interface system, fig. 11 shows the output noise power spectral density which is  $6 \mu V/\sqrt{Hz}$ , corresponding to  $15 nV/\sqrt{Hz}$  at the input. The equivalent input offset versus a tuning error between the bandpass resonance frequency and the chopper frequency is depicted in fig. 12. The influence of the thermopile resistance on the offset is shown in fig. 13. To test the performance of the system the amplifier and one sensor have been connected together. The sensor has been exposed to a 3 Hz chopped IR radiation of  $120 nW/mm^2$  which is the minimum required detectable radiation. The preamplified signal has been further amplified and low-pass filtered externally. The total gain is  $400 \times 25$ , filter cut-off is at 10 Hz. The resulting measured time response is shown in fig. 14. The sensor signal at the input of the interface amplifier corresponds to only  $650 nV$ . Dividing this value by the number of thermocouples  $N = 64$  and the Seebeck coefficient  $\alpha$  of  $108 \mu V/K$  for this process, an equivalent temperature difference of only  $94 \mu K$  between membrane and silicon bulk is detected. The amplified signal allows an easy detection using a schmitt-trigger circuit. The additional offset ( $\approx 38 \mu V$  at the input of the interface amplifier) is in disaccordance with the experimental values measured in fig. 13 and is due to the background radiation. However, as is the case for detector applications, a second sensor will be differentially connected in the final design such that common mode radiation will be suppressed.

## Conclusion

A highly sensitive sensor interface for low noise thermoelectric IR sensors has been built in a transistor-only, digital  $1 \mu m$  CMOS process. It features very low offset, low noise and low power consumption. Measurements show that the resulting microsystem can easily detect the minimum required radiation. This contribution proves the feasibility of high performance sensor systems using an inexpensive process.

## Acknowledgement

This work was supported by the European research program ESPRIT, contract Nr. 8756 (DEMAC)

## References

- [1] N. Schneeberger, S. Déteindre, O. Paul, and H. Baltes, "Optimized CMOS infrared detector microsystems", in *Proc. of TENCON, IEEE Asia*, Hong Kong, November 1995, pp. 198–201.
- [2] R. C. Yen and P. R. Gray, "A MOS switched-capacitor instrumentation amplifier," *IEEE J. Solid-State Circuits*, vol. SC-17, pp. 1008–1013, Dec 1982.
- [3] M. Degrauwe, E. Vittoz, I. Verbauwhede, "A micropower CMOS-instrumentation amplifier," *IEEE J. Solid-State Circuits*, vol. SC-20, pp. 805–807, June 1985.
- [4] K.-C. Hsieh, P. R. Gray, D. Senderowicz, and D. G. Messerschmitt, "A low-noise chopper-stabilized differential switched-capacitor filtering technique," *IEEE J. Solid-State Circuits*, vol. SC-16, pp. 708–715, Dec 1981.
- [5] C. Enz, E. Vittoz, F. Krummenacher, "A CMOS chopper amplifier," *IEEE J. Solid-State Circuits*, vol. SC-22, pp. 335–342, June 1987.
- [6] F. Krummenacher, N. Joehl, "A 4-MHz CMOS continuous-time filter with on-chip automatic tuning," *IEEE J. Solid-State Circuits*, vol. SC-23, pp. 750–758, June 1988.

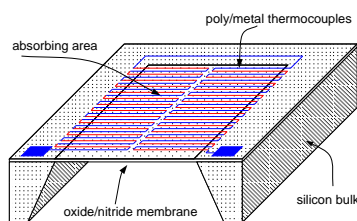


Figure 1: Schematic structure of the CMOS IR sensor

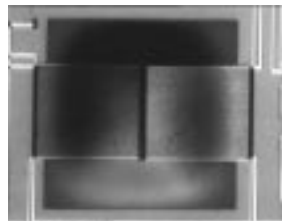


Figure 2: Photograph of the sensor membrane

Membrane Size	$600 \times 600 \mu m^2$
Number of Thermocouples	64
Thermopile Resistance	$100 k\Omega$
Sensitivity	$15 V/W$
Noise eq. Input Power	$2.8 nW/\sqrt{Hz}$

Figure 3: Specifications of the sensor used for the intrusion detector

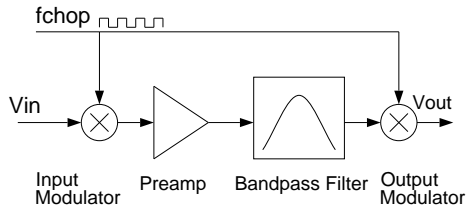


Figure 4: Block diagram of the interface

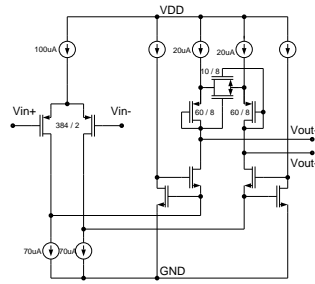


Figure 5: Preamplifier

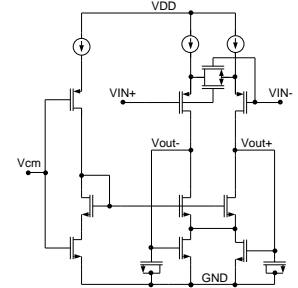


Figure 6: Integrator

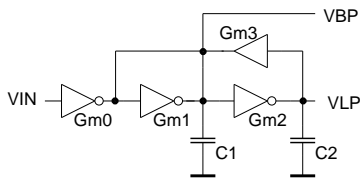


Figure 7: Bandpass filter

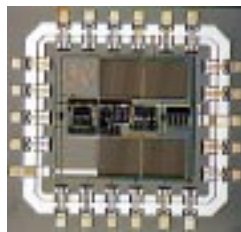


Figure 8: Chip photograph of the interface circuit

Supply voltage	5 V
Power consumption	1.3 mW
DC gain	410 ± 3%
Bandwidth	500 Hz
CMRR (up to 100 kHz)	> 70 dB
PSRR - (at $f_{chop}$ )	> 60 dB
PSRR + (at $f_{chop}$ )	> 70 dB
Input offset for ± 4 % tuning error	± 1.5 μV
Equivalent low frequency input noise PSD	15 nV/√Hz
THD, $\hat{V}_{in} = 500 \mu V$	0.18 %
THD, $\hat{V}_{in} = 2 mV$	0.6 %

Figure 9: Measured amplifier performance

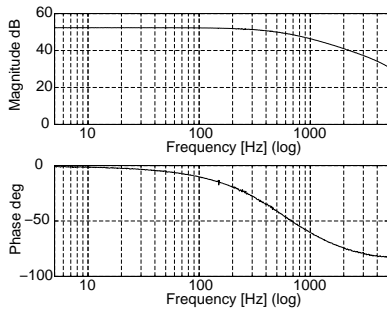


Figure 10: Amplifier frequency response

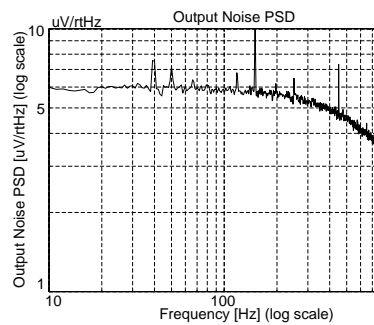


Figure 11: Output noise PSD

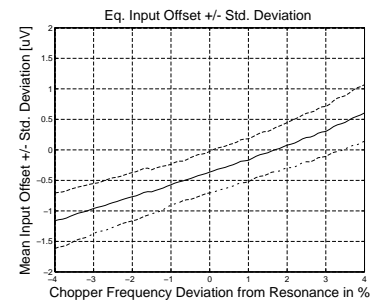


Figure 12: Offset performance of the interface,  $R_T = 0 \Omega$

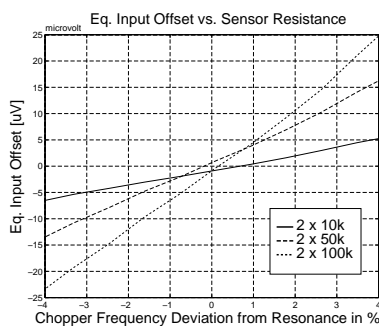


Figure 13: Eq. Input offset versus thermopile resistance

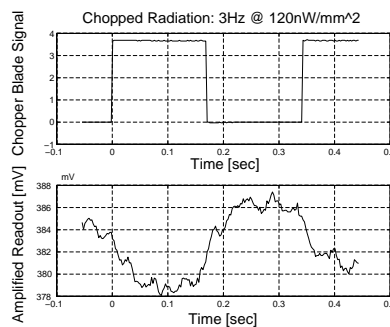


Figure 14: Sensor response at  $120 \text{ nW/mm}^2$  radiation, bandwidth limited to 10 Hz, total gain  $400 \times 25$

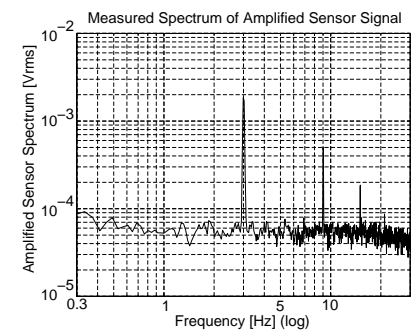


Figure 15: Spectrum of the sensor response at  $120 \text{ nW/mm}^2$  radiation